

## Article

# A Use-Store-Reuse (USR) Concept in Catalytic HCOOH Dehydrogenation: Case-Study of a Ru-Based Catalytic System for Long-Term USR under Ambient O<sub>2</sub>

Marinos Theodorakopoulos <sup>1</sup>, Maria Solakidou <sup>2</sup>, Yiannis Deligiannakis <sup>2,3</sup> and Maria Louloudi <sup>1,3,\*</sup>

<sup>1</sup> Laboratory of Biomimetic Catalysis and Hybrid Materials, Department of Chemistry, University of Ioannina, GR45110 Ioannina, Greece; m.theodorakopoulos@uoi.gr

<sup>2</sup> Laboratory of Physical Chemistry of Materials and Environment, Department of Physics, University of Ioannina, GR45110 Ioannina, Greece; maria-sol@windowslive.com (M.S.); ideligia@uoi.gr (Y.D.)

<sup>3</sup> Institute of Environment & Sustainable Development, University Research Center of Ioannina, GR45110 Ioannina, Greece

\* Correspondence: mlouloud@uoi.gr; Tel.: +30-2651008418

**Abstract:** Commercial use of H<sub>2</sub> production catalysts requires a repeated use/stop/store and reuse of the catalyst. Ideally, this cycle should be possible under ambient O<sub>2</sub>. Herein we exemplify the concept of Use-Store-Reuse (USR) of a (Ru-phosphine) catalyst in a biphasic catalytic system, for H<sub>2</sub> production *via* dehydrogenation of HCOOH. The catalytic system can operate uninterrupted for at least four weeks, including storage and reuse cycles, with negligible loss of its catalytic efficiency. The catalytic system consisted of a RuP(CH<sub>2</sub>CH<sub>2</sub>PPh<sub>2</sub>)<sub>3</sub> (i.e. RuPP3) in (*tri*-glyme/water) system, using KOH as a cocatalyst, to promote HCOOH deprotonation. In a USR cycle of 1 week, followed by storage for three weeks under ambient air and reuse, the system achieved in total TONs > 90,000 and TOFs > 4000 h<sup>-1</sup>. Thus, for the first time, a USR concept with a readily available stable ruthenium catalyst is presented, operating without any protection from O<sub>2</sub> or light, and able to retain its catalytic performance.

**Keywords:** hydrogen; Use-Store-Reuse (USR); long-term operation (LTO); ruthenium complex; phosphine ligand



**Citation:** Theodorakopoulos, M.; Solakidou, M.; Deligiannakis, Y.; Louloudi, M. A Use-Store-Reuse (USR) Concept in Catalytic HCOOH Dehydrogenation: Case-Study of a Ru-Based Catalytic System for Long-Term USR under Ambient O<sub>2</sub>. *Energies* **2021**, *14*, 481. <https://doi.org/10.3390/en14020481>

Received: 28 December 2020

Accepted: 14 January 2021

Published: 18 January 2021

**Publisher's Note:** MDPI stays neutral with regard to jurisdictional claims in published maps and institutional affiliations.



**Copyright:** © 2021 by the authors. Licensee MDPI, Basel, Switzerland. This article is an open access article distributed under the terms and conditions of the Creative Commons Attribution (CC BY) license (<https://creativecommons.org/licenses/by/4.0/>).

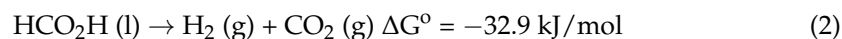
## 1. Introduction

Nowadays, fossil fuels & natural gas constitute the main sources of energy production [1]. Drawbacks regarding these resources relate to cost and environmental impact, i.e., air pollution and CO<sub>2</sub> emission [2]. So far, molecular hydrogen (H<sub>2</sub>) has emerged as a highly promising alternative towards clean energy production [3,4], due to its high energy (2.6 higher than gasoline) and storage density (120 MJ kg<sup>-1</sup>). A strategic advantage of H<sub>2</sub> use is that its combustion or fuel-cell utilization produces H<sub>2</sub>O as a sole byproduct [5,6]. The most promising methods for chemical-storage of H<sub>2</sub> include liquid organic hydrogen-carriers (LOHCs) [7], under the condition that they would allow for a cost-efficient release of H<sub>2</sub>, i.e., via an efficient catalytic reaction. At present, the most attractive LOHCs include C1 hydrocarbons such as methanol, formaldehyde, and formic acid [8].

Specifically, Formic Acid (FA), is gaining a lot of attention in the scientific community as a promising route for H<sub>2</sub> storage and release at competitive technology-readiness levels, i.e., under mild P, T conditions, and for its high gravimetric (4.4 wt.%) and volumetric (53.4 g/L) capacity [9–11].

The decomposition of FA can proceed via two possible paths [12], as described by Reaction Equations (1). Reaction Equation (1) has to be prevented, i.e., because CO is poisonous to the fuel-cells. The desired reaction path in Equation (2) is thermodynamically

allowed,  $\Delta G^\circ = -32.9$  kJ/mol at high temperatures, however, is kinetically limited [13], thus a catalyst is needed to accelerate it.

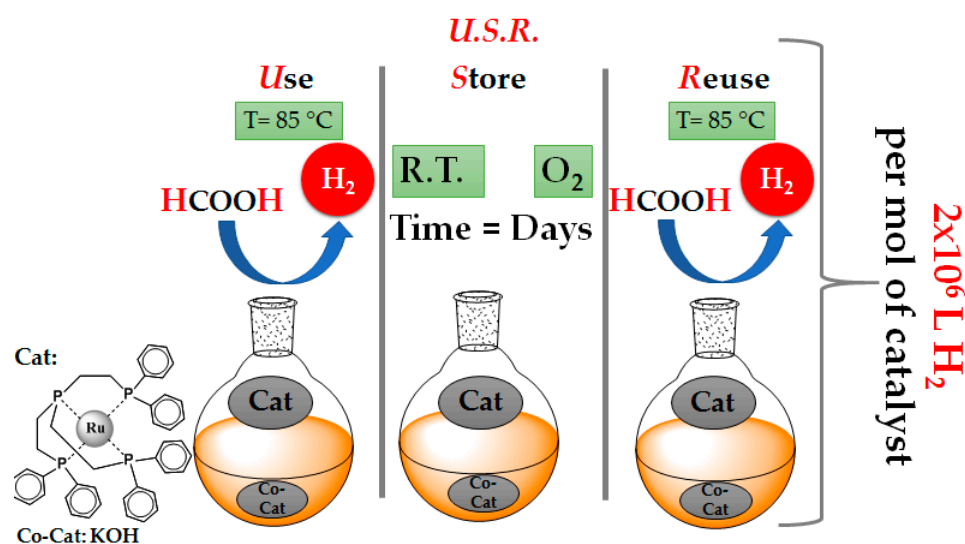


Since 1967 when Coffey and his group published on the first Ir/Phosphine catalytic complex [14], much research works has been reported on dehydrogenation of FA, using homogeneous catalysts. In 2008, Beller et al. reported an efficient ruthenium catalyst, with the addition of a base as co-catalytic-additive, achieving TOFs =  $301 \text{ h}^{-1}$  [15]. Laurenczy et al., in 2009, presented a water-soluble  $(\text{Ru}(\text{H}_2\text{O})_6)^{2+}$ /TPPTS complex, achieving a TOF value of  $444 \text{ h}^{-1}$  [16]. In 2016, Huang et al. [17] presented a catalytic  $(\text{Ru}/\text{PN}^3\text{-pincer})$  complex in DMSO and DMF solvents; using triethylamine ( $\text{Et}_3\text{N}$ ) and  $\text{Na}_2\text{CO}_3$  as co-catalytic-additives, this system achieved TOFs of  $13,123 \text{ h}^{-1}$  and  $31,000 \text{ h}^{-1}$ , respectively [17]. A novel route for the dehydrogenation of formic acid was introduced by Beller et al. [18] using  $(\text{Fe}(\text{BF}_4)_2) \cdot 6\text{H}_2\text{O}$  as metal-precursor and *tris*((2-diphenylphosphino)ethyl)phosphine ( $\text{P}(\text{CH}_2\text{CH}_2\text{PPh}_2)_3$  or PP3) as a phosphine ligand, achieving TOFs =  $1962 \text{ h}^{-1}$  in propylene carbonate at  $60^\circ\text{C}$ , without any base additive [18]. Recently, we have exemplified that  $\text{SiO}_2$  nanoparticles can act as a very efficient co-catalyst for a  $\text{Fe}/(\text{P}(\text{CH}_2\text{CH}_2\text{PPh}_2)_3)$  complex [19]. This heterogeneous system achieved TOFs =  $13,882 \text{ h}^{-1}$ , which is >10 times higher than the TOF of the corresponding homogeneous system (TOFs =  $1205 \text{ h}^{-1}$ ), without the co-catalyst [19].

Despite the encouraging progress in enhancing TOFs of  $\text{H}_2$ -production catalysts, the long-term operation of a given catalyst remains a standalone challenge. This will have to be faced shortly when technology-readiness will require to advance beyond  $\text{H}_2$ -production rates towards catalysts' storage-reuse demands. In 2018, we described a phenomenon where amines grafted on  $\text{SiO}_2$  nanoparticles, i.e.,  $\text{NH}_2@/\text{SiO}_2$  nano hybrids, provided a significant efficiency/stability boost to a  $\text{Ru}(\text{PP3})$  catalyst [19]. Specifically, using  $(\text{FA}:\{\text{NH}_2 \text{ grafted on } \text{SiO}_2\})$  at ratio (500:1) the system  $\text{Ru}(\text{PP3})/\text{NH}_2@/\text{SiO}_2$  achieved TOFs =  $510 \text{ h}^{-1}$  for uninterrupted operation over >16 h, under a continuous supply of formic acid [20]. Along the same lines, recently we demonstrated that "double-ligand" catalysts, e.g.,  $\text{Ru}/\text{PP3}/\text{L}\gamma$  and  $\text{Fe}/\text{PP3}/\text{L}\gamma$  together with the  $\text{NH}_2@/\text{SiO}_2$  co-catalytic particles, were able to operate under a continuous FA feed, achieving remarkable total TONs of  $6679 \text{ h}^{-1}$  and  $11,296 \text{ h}^{-1}$ , respectively [21].

Given that most of the catalytic systems suffer from a rather rapid deactivation of the catalyst and poor long-term stability performance, the development of stable catalysts under long-term applications, i.e., at a commercial level, is an appealing challenge. Within this context, so far, some efforts have been realized towards the development of continuous operating systems. This approach had been pioneered by Beller's group, who had exemplified a long-term stability  $(\text{RuCl}_2(\text{benzene}))_2/\text{dppe}$  system, i.e., for a 30 h operating time [22]. Using as a base (*N,N*-dimethyl-*n*-hexylamine), they have reported a TOF~ $2000 \text{ h}^{-1}$  [22]. Gonsalvi et al. [23] presented a Ru-tetra-phosphine-based catalytic system with a {*meso*-1,1,4,7,10,10-hexaphenyl-1,4,7,10-tetraphosphadecane} as ligand, in propylene carbonate solvent. Under a continuous formic acid feed, their system achieved TOFs =  $4600 \text{ h}^{-1}$  at  $60^\circ\text{C}$  after 48 h; however, the system was sensitive to  $\text{O}_2$ , thus it required an  $\text{N}_2$  atmosphere [23]. Huang et al. [24] used a water-soluble  $(\text{Ru}/\text{N,N}'\text{-diamine})$  complex, operating under a continuous FA/ $\text{HCOONa}$  feed. This system required high-pressure conditions achieving TOFs =  $12,000 \text{ h}^{-1}$  after 30 h [24]. A catalytic system  $(\text{Ru}(\text{H})(\text{Cl})(\text{CO})(\text{CH}_3\text{N}(\text{CH}_2\text{CH}_2\text{P}(\text{iPr})_2)_2))$  in tri-glyme/water and KOH as a base-additive, was reported to achieve TOF =  $4400 \text{ h}^{-1}$  in 6 h under an argon atmosphere [25]. We underline that, in all the reported previous works, the uninterrupted long-term operation of the catalyst required operation under a strictly non-ambient atmosphere, i.e., exclusion of  $\text{O}_2$  by an inert gas, to avoid the decomposition of the catalytic complexes [22–24].

Herein, we present the first example of a Ru-catalytic system that can operate under long-term conditions under atmospheric  $O_2$ , schematically depicted in Scheme 1. The catalytic system comprises of a (Ru-PP<sub>3</sub>) complex in a tri-glyme/water solution which contains formic acid partially deprotonated by KOH. As we show herein, this catalytic system was able to operate for seven sequential days under daily storage and reuse, followed by a three weeks storage and reuse. Remarkably, the catalytic system was active after one month showing a decrease of ~10% of its catalytic activity.



**Scheme 1.** Concept of U.S.R. (i.e., Use-Store-Reuse) technology. The catalytic system is set for  $H_2$ -production at  $T = 85\text{ }^{\circ}\text{C}$  (Use), stored under ambient P, T,  $O_2$  (Store), and Reused at  $T = 85\text{ }^{\circ}\text{C}$ . The system during the whole operation (weekly and monthly) produced  $>2 \times 10^6$  L of  $H_2$  per mole of catalyst.

## 2. Materials and Methods

### 2.1. Materials

FA (purity 97.5% with 2.5%  $H_2O$ ),  $(RuCl_3 \cdot (H_2O)_x)$  (ruthenium-III chloride hydrate, content 40.0–49.0%, purity 98%), Tris (2-(di-phenyl-phosphine)ethyl)phosphine ( $P(CH_2CH_2PPh_2)_3$ ) (PP<sub>3</sub>) (98% purity), were purchased from Sigma Aldrich and kept under Ar atmosphere. Tri-ethylene glycol dimethyl ether (tri-glyme) solvent and KOH pellets ( $\geq 85\%$ ) were obtained from Merck.

### 2.2. Catalytic Procedures

Catalytic activity was evaluated in the same protocols as previous works [20]. In a typical catalytic experiment, 2 mg (9  $\mu\text{mol}$ ) of  $(RuCl_3 \cdot (H_2O)_x)$  and 13.4 mg (20  $\mu\text{mol}$ ) of  $P(CH_2CH_2PPh_2)_3$  (PP<sub>3</sub>) were dissolved in 2 mL tri-glyme solvent. The maximum incubation time for the formation of (Ru-phosphine) complex was 10 min (mixture 1, pre-catalyst) [20]. A solution of 2 mL formic acid (48 mmol), 1 mL water, 8 mL tri-glyme, and 0.55 g KOH (10 mmol) was heated in a glass reactor (mixture 2) at  $85\text{ }^{\circ}\text{C}$  for 20 min. Then, the pre-catalyst solution was added into the reactor (mixture 2) setting the starting point of the catalytic reaction. The volume of the evolving gas mixture was measured manually or by an automatic burette setup [20]. In all cases after the addition of (Ru-phosphine) (pre-catalyst) into mixture 2, the gas evolution was observed immediately. Quantification of produced gases was realized, directly after the addition of FA, inside an automatic gas burette at ambient atmosphere. The analysis of  $H_2$  and  $CO_2$  was made by a Shimadzu GC-2014 Gas Chromatograph combined with TCD detector and Carboxen-1000 column [20].

### 2.3. Characterization Techniques

Attenuated Total Reflection-FTIR (ATR-FTIR) experiments were recorded in situ, in the region of 400–2000  $\text{cm}^{-1}$  by an Agilent spectrometer including a ZnSe-attenuated total reflection accessory. Raman measurements were performed with a Xplora one System Horiba PLUS instrument which employed an argon-ion laser at 532 nm diode as excitation source, from a range of 540 to 2000  $\text{cm}^{-1}$ . A liquid sample from the in-situ experiments was drop-casted on KBr pellets

## 3. Results and Discussion

### 3.1. Operation Mode and Catalytic Data

The set-up of the optimum functional catalytic system used in this work includes the in situ formation of the (Ru-PP3) pre-catalyst with a molar ratio of (Ru):(PP3) = 1:2 and its addition in a water/tri-glyme ( $v/v = 1:8$ ) solution, containing 2 mL of FA and 10 mmol of KOH which were added to promote deprotonation of a fraction of HCOOH. The catalytic systems derived from a molar ratio of (Ru):(PP3) equal to 1:1, 1:3, 1:4, and 1:5 have also been studied and the obtained data are provided in the Supplementary Materials (See Tables S1 and S2). We should underline that, in the 1:1 ratio, the complex has optimal activity. In catalysis, the existence of available non-occupied coordination sites is required in order to be active. To achieve the formation of the active complex 1:1 (Ru/PP3) in situ in all centers, we have added the second ligand in excess. Screening experiments showed that the optimum amount of KOH was 10 mmol, i.e., higher concentrations did not affect the  $\text{H}_2$  production rate. Gas GC-TCD analysis showed that during the whole catalytic procedure the only gases produced from FA decomposition were  $\text{H}_2$  and  $\text{CO}_2$  in the ratio 1:1 (Figure S1).

*Daily operation:* The catalytic procedure for one day was carried out as follows: addition of (Ru-PP3) (pre-catalyst) into the reactor which contains 2 mL of partially deprotonated FA at 85 °C, (see Scheme 1), initiated the catalytic reaction followed immediately by gas evolution. After the added FA was consumed (1ml of FA produces about 1.2 L of total gasses) another dose of FA (1 mL) was added and the system maintained the gasses' production. After the addition of 5 sequential doses of FA (each dose 1 mL of FA, total 5 mL FA), the system was cooled down and kept in ambient conditions, without any protection against ambient oxygen or daily light.

*Weekly operation:* To restart the catalytic  $\text{H}_2$ -production, i.e., next day, it was required to add only a new dose of FA (1 mL) and to reset the heating at 85 °C. In the same way, when the added FA was consumed, another dose of FA was added, and so on. After 5 added doses of FA (5 mL) were decomposed towards the production of gasses, the reactor was cooled down and kept in ambient conditions without any additional care. This process was carried out for seven sequential days.

*Monthly operation:* After the catalytic system had accomplished a weekly operation as described above, it was put in standby mode by cooling, with no FA added, under ambient P, T, for 3 weeks. Then, a month after the first operation of the catalytic system, a new dose of FA (1 mL) was added and upon heating at 85 °C the production of gasses started over again. Then, when the FA was consumed, another dose of FA was introduced into the reactor and so on, till 5 successive doses of FA had been added. The total volume of gasses produced from catalytic decomposition of FA by the (Ru/PP3) per day is presented in Table 1 and Figure 1. Each entry in Table 1 represents an operating day of the catalytic system. On Entry 1 the catalytic system decomposed in total 5 mL of FA (2 mL at the beginning, plus three additional doses of 1 mL each), providing in total 5.1 L of gas within 110 min and achieving TONs = 11,468 and TOFs = 6267. During the second operation day (Entry 2), the same amount of FA (5 mL) was consumed within the same period (110 min), producing 5.12 L of gasses with TONs = 11,513 and TOFs = 6291  $\text{h}^{-1}$ . In the same manner in Entry 3 and 4, the catalytic system maintained the same reactivity, where the produced gas volume was 5.18 L in 110 min with TONs = 11,648 and TOFs = 6365  $\text{h}^{-1}$ , and 5.25 L with TONs = 11,806 and TOFs = 6451  $\text{h}^{-1}$  correspondingly. On the fifth operational day,

the catalytic system showed slight fatigue, since it required 140 min to consume 5 mL of FA; however, it produced the same volume of gasses (5.11 L) with analogous TONs (11,491), but with reduced TOFs = 4931 h<sup>-1</sup>. For the next two days, the catalytic system showed an analogous functional profile as on the 5th day, i.e., 6th day: FA (5 mL), reaction time (140 min), gas volume (5.1 L), TONs = 11,468, TOFs = 4922 h<sup>-1</sup>; 7th day: 5 mL of FA, reaction time (140 min), gas volume (5.2 L), TONs = 11,693, TOFs = 5018 h<sup>-1</sup>. As mentioned above, after this operation the catalytic system was left at ambient conditions for 23 days and the catalytic system was retested for its ability to decompose FA. Thus, it was observed that it was able to produce 4.5 L of gasses from 5 mL of FA within 240 min with TONs = 10,119 and TOFs = 2529 h<sup>-1</sup> (Table 1, Figure 1). From the above description, it is clearly demonstrated that the catalyst (Ru/PP3) remains unimpaired, showing a steady activity for a whole week, with gas production of 5.2 L/day, thus 36.0 L in total after a total operation time of 14.3 h (Figure 1b). At this point, it is underlined that, a month after the first use of the catalyst, it remained active, producing 4.5 L of gasses, i.e., a decline of catalytic performance of 13% vs. its initial performance. After the 5th operation day, the kinetics of H<sub>2</sub> production showed a slight delay (see Figure 1a). This is reflected in the rate of gas production that was 70–80 mL/min for the first four operation days, vs. 50 mL/min measured on the 7th day, vs. 30 mL/min after a month (see Figure S2). The TOFs showed analogous trends i.e., as visualized in Figure 2 which presents the overall trends of TONs and TOFs values vs. operation days. The data in Figure 2 demonstrate the long-term stability and durability of the studied system, which accomplished up to 90,000 TONs. We should underline that a marginal diminution of 13% occurs only in the case of TOF (manifested by a drop in the catalytic rate). The TONs indicator remains just the same. This could be attributed to a minor deactivation of the catalyst, but the exact reason should be further investigated. Up to this point, the Electron Paramagnetic Resonance data (Supplementary material, Figure S4, spectrum (iv)) shows no Ru<sup>II</sup> oxidation at the end of the reaction. Moreover, the formation of Ru-carbonyls could be confirmed via Raman and ATR spectroscopies, something that in our study is excluded. Another less plausible explanation could be the accumulation of water after the sequential additions of FA (2.5% (v:v) is contained in the FA stock, as obtained from the supplier). The same phenomenon was observed in similar studies [26,27].

**Table 1.** Catalytic data for formic acid (FA) decomposition by (9 μmol) of (Ru/PP3) in tri-glyme:water [v/v = 10:1] solution at 85 °C.

Entry *	FA Added (mL)	Produced Gas Volume (L)	TONs	TOFs (h <sup>-1</sup> )	Reaction Time (min)
1	5	5.10	11,468	6267	110
2	5	5.12	11,513	6291	110
3	5	5.18	11,648	6365	110
4	5	5.25	11,806	6451	110
5	5	5.11	11,491	4931	140
6	5	5.10	11,468	4922	140
7	5	5.20	11,693	5018	140
30	5	4.50	10,119	2529	240

\* Each Entry represents the operating day of the catalytic system.

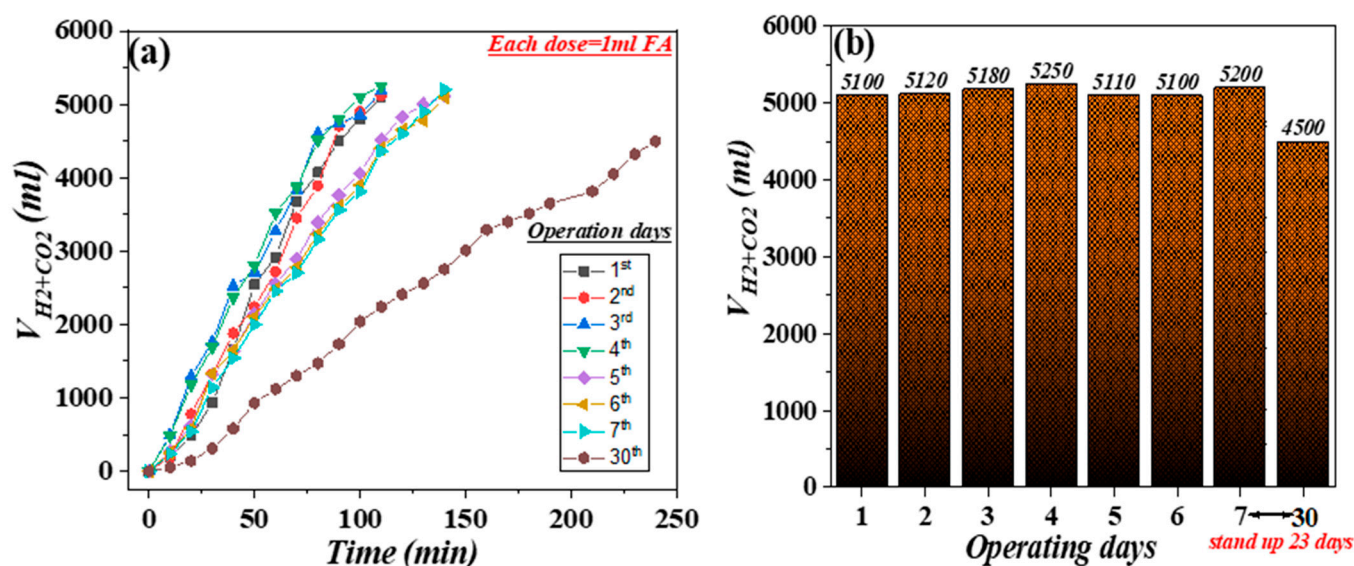


**Figure 1.** (a) Kinetics of gas production and (b) total gas volume produced every operation's day. Conditions: (Ru/PP3) (9  $\mu$ mol) in tri-glyme:water (v/v = 10 mL:1 mL) solution which contained FA and 10 mmol of KOH at 85  $^{\circ}$ C.

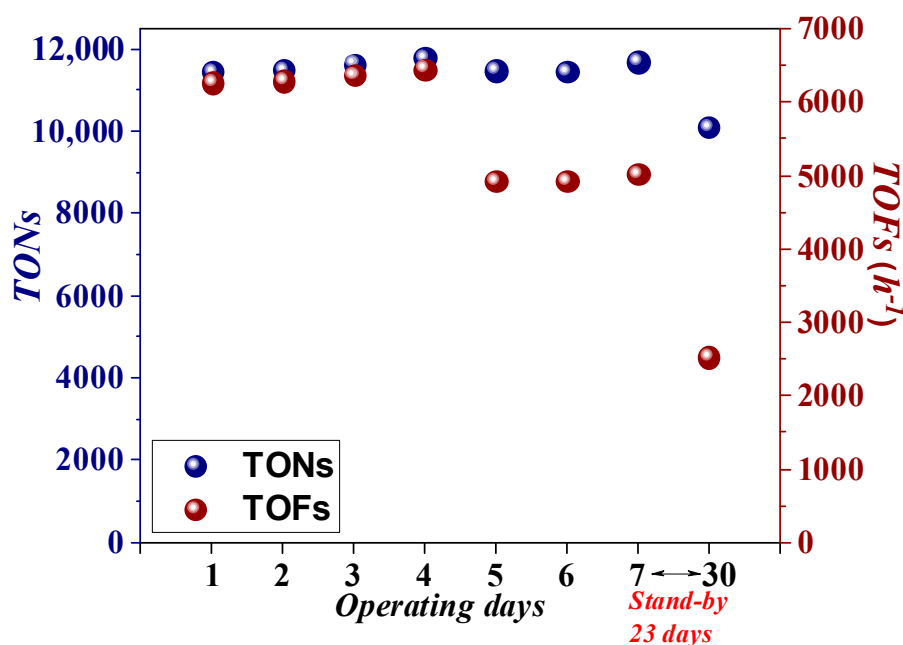


**Figure 2.** TONs and TOFs measured on each operation day. Conditions: (Ru/PP3) (9  $\mu$ mol) in tri-glyme:water (v/v = 10 mL:1 mL) solution which contained FA and 10 mmol of KOH at 85  $^{\circ}$ C.

### 3.2. Spectroscopic Study of Catalysis In Situ

A more detailed study of the catalytic reaction, was realized using *in situ* ATR, Raman, and EPR spectroscopies. The obtained Raman and ATR spectra are provided in Figures 3 and 4, respectively, where each one shows the spectrum of (a) tri-glyme solvent, (b) PP3 ligand, (c) [Ru-PP3] catalyst in tri-glyme, and (d) the full catalytic reaction system (Ru-PP3)/FA/KOH/tri-glyme:water solution (v/v = 10/1).

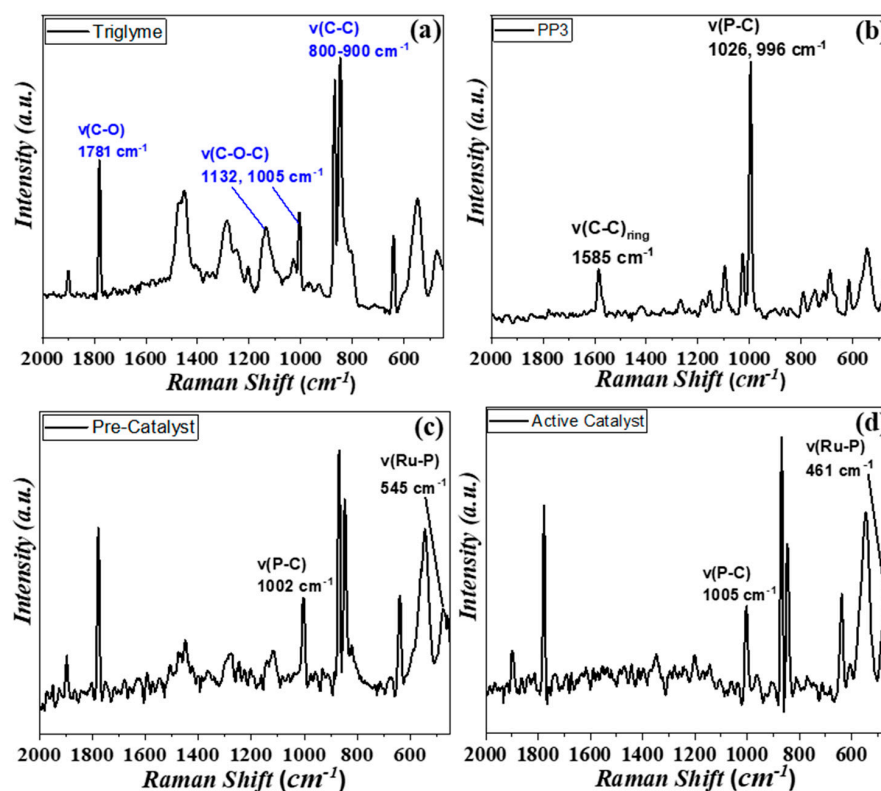


Figure 3. Raman spectra of (a) tri-glyme (solvent), (b) phosphine ligand (PP3), (c) (Ru/PP3) catalyst in tri-glyme and (d) catalytic reaction ( $[\text{Ru}/\text{PP3}]/\text{FA}/\text{KOH}$  in tri-glyme: water solution).

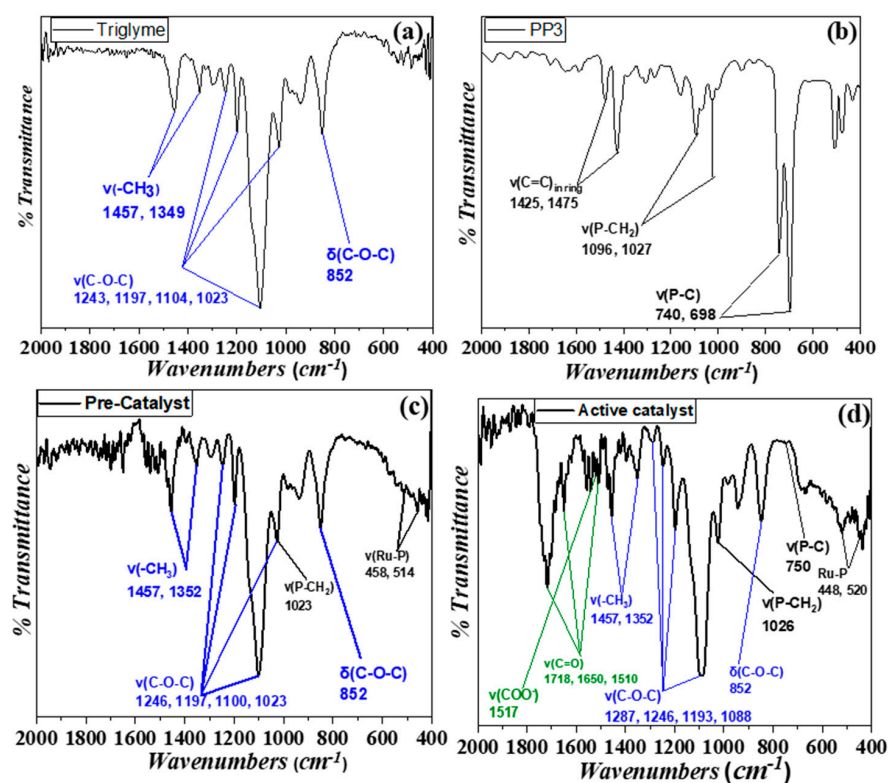


Figure 4. ATR-FTIR spectra of (a) tri-glyme (solvent), (b) phosphine ligand (PP3), (c)  $[\text{Ru}/\text{PP3}]$  catalyst in tri-glyme and (d) catalytic reaction ( $(\text{Ru}/\text{PP3})/\text{FA}/\text{KOH}$  in tri-glyme: water solution).

The  $\nu(\text{C-C})$ ,  $\nu(\text{C-O-C})$ , and  $\nu(\text{C-O})$  vibrations in the Raman spectra (see Figure 3a) and the  $\delta(\text{C-OC})$ ,  $\nu(\text{C-O-C})$ , and  $\nu(-\text{CH}_3)$  bands in the ATR spectra (see Figure 4a) are attributed to the tri-glyme solvent. The intense frequency shifting, from  $545\text{ cm}^{-1}$  to  $461\text{ cm}^{-1}$  (Ru-P Stretching), and from  $996\text{ cm}^{-1}$  to  $1002\text{ cm}^{-1}$  and  $1006\text{ cm}^{-1}$ , (P-C stretching bond) are attributed to the formation of the catalytic complex (Ru/PP3) (Figure 3c,d respectively).

The formation of the (Ru/PP3) complex and its presence in the catalytic reaction are affirmed by the ATR data, where the peaks at  $468\text{ cm}^{-1}$  and  $514\text{ cm}^{-1}$  in Figure 4c, and those at  $448\text{ cm}^{-1}$  and  $520\text{ cm}^{-1}$  in Figure 4d are attributed to the stretching Ru-P bond. Moreover, the EPR data confirm the formation of the  $\text{Ru}^{\text{III}}/\text{PP3}$  complex, (see signal (ii) in Figure S4). The EPR spectrum is a characteristic  $S = 1/2$  low spin signal which confirms the oxidation state of  $\text{Ru}^{\text{III}}$  [20,21]. The addition of the catalyst (Ru/PP3) in tri-glyme/water solution, which contained  $\text{HCOO}^-$  anions, i.e., due to  $\text{HCOOH}$  deprotonated by  $\text{KOH}$ , contributes to the diminution of the EPR signal (see spectrum (iii) in Figure S4), while, at the end of the catalytic reaction, the EPR signal of  $\text{Ru}^{\text{III}}$  dropped to zero (see spectrum (iv) in Figure S4  $\text{Ru}^{\text{III}}$ ). This is due to the reduction of  $\text{Ru}^{\text{III}}$  to  $\text{Ru}^{\text{II}}$ , which is EPR silent [21]. At this point, we should mention that when the catalytic reaction was restarted, the EPR data (signal (v), Figure S4) did not show any oxidized  $\text{Ru}^{\text{III}}$ -species, thus confirming the stability of the formed active  $\text{Ru}^{\text{II}}$ -catalyst.

When the catalytic reaction was monitored by ATR spectroscopy (see Figure 4d), the three characteristic bands at  $1718$ ,  $1650$ , and  $1510\text{ cm}^{-1}$  are attributed to the stretching of the  $\text{C=O}$  bond of FA, while the band observed at  $1517\text{ cm}^{-1}$  is due to the stretching bond of the  $\text{HCOO}^-$  anion. These bonds also refer to the  $\eta^1\text{-O}_2\text{CH}$  and  $\eta^2\text{-O}_2\text{CH}$  modes of formic acid coordinated to the metal center [21,28]. According to previous studies [12,18,29], two possible catalytic cycles could be involved in the dehydrogenation of  $\text{HCOOH}$ , using a molecular homogeneous complex. In brief, Cycle-1 initiates with a  $\text{HCOO}^-$  anion and one  $\text{HCOOH}$  molecule, while Cycle-2 start with a  $\text{HCOO}^-$  anion in addition to a second formate anion ( $\text{HCOO}^-$ ). We should mention that in both cases the involvement of  $\beta$ -hydride transfer from substrate to metal is the critical step. Yang, in his computational study, mentioned that Cycle-2 is less thermodynamically favorable than Cycle-1 [30]. Indeed, in most of the surveys, it is proposed that the involvement of a  $\text{HCOO}^-$  anion is more possible than the insertion of a  $\text{HCOOH}$  molecule [20,24,31,32].

#### 4. Conclusions

In this work, we present the first example of the USR concept, using a (Ru-PP3) catalyst in tri-glyme. Raman, ATR, and EPR spectroscopies confirm that an initial key step is a reduction of ( $\text{Ru}^{\text{III}}\text{-PP3}$ ) to ( $\text{Ru}^{\text{II}}\text{-PP3}$ ) which remained stable during catalysis with the involvement of FA.

The catalytic system was able to completely decompose five sequential doses of FA without the need for an additional  $\text{KOH}$  base. After, the reaction was stopped, stored (storage) at ambient conditions, and restarted (reuse) at will, with the addition only of a new amount of FA and reheating. These repetitive use/storage/reuse (USR) cycles occurred for a whole week, under ambient air, i.e., without any defense against atmospheric  $\text{O}_2$  and light. During this weekly operation, the catalytic system was completely active achieving 81,090 TONs with TOFs  $5670\text{ h}^{-1}$ . To test the system's stability and durability, we stored it for an additional three weeks without any protection and the catalytic production was re-initiated by the addition of formic acid and heating.

Overall, the present work exemplifies the feasibility of the USR technology with a readily available, easy to handle, catalytic system.

**Supplementary Materials:** The following are available online at <https://www.mdpi.com/1996-1073/14/2/481/s1>.

**Author Contributions:** Conceptualization, M.L.;  $\text{H}_2$  production, M.T.; EPR spectroscopy, M.S.; Writing—original draft preparation, M.T. and M.L.; writing—review and editing, Y.D. and M.S.; supervision, M.L.; All authors have read and agreed to the published version of the manuscript.

**Funding:** This research received no external funding.

**Institutional Review Board Statement:** Not applicable.

**Informed Consent Statement:** Not applicable.

**Data Availability Statement:** Not applicable.

**Conflicts of Interest:** The authors declare no conflict of interest.

## References

1. Jacobson, M.Z. Review of solutions to global warming, air pollution, and energy security. *Energy Environ. Sci.* **2009**, *2*, 148–173. [[CrossRef](#)]
2. Hansen, J. Climate sensitivity: Analysis of feedback mechanisms. *Clim. Process. Clim. Sensit.* **1984**, *5*, 130–163.
3. Andreas, Z.; Borgschulte, A. *Handbook of Fuels Beyond Oil and Gas: The Methanol Economy Molten Carbonate Fuel Cells*, 1st ed.; Wiley-VCH: Weinheim, Germany, 2007; ISBN 9783527307401.
4. Elam, C.C.; Padró, C.E.G.; Sandrock, G.; Luzzi, A.; Lindblad, P.; Hagen, E.F. Realizing the hydrogen future: The International Energy Agency's efforts to advance hydrogen energy technologies. *Int. J. Hydrogen Energy* **2003**, *28*, 601–607. [[CrossRef](#)]
5. Amende, M.; Kaftan, A.; Bachmann, P.; Brehmer, R.; Preuster, P.; Koch, M.; Wasserscheid, P.; Libuda, J. Regeneration of LOHC dehydrogenation catalysts: In-situ IR spectroscopy on single crystals, model catalysts, and real catalysts from UHV to near ambient pressure. *Appl. Surf. Sci.* **2016**, *360*, 671–683. [[CrossRef](#)]
6. Jörissen, L. Hydrogen and Fuel Cells. Fundamentals, Technologies and Applications. Edited by Detlev Stolten. *Angew. Chem. Int. Ed.* **2011**, *50*, 9787. [[CrossRef](#)]
7. Aakko-Saksa, P.T.; Cook, C.; Kiviaho, J.; Repo, T. Liquid organic hydrogen carriers for transportation and storing of renewable energy—Review and discussion. *J. Power Sources* **2018**, *396*, 803–823. [[CrossRef](#)]
8. Crabtree, R.H. Hydrogen storage in liquid organic heterocycles. *Energy Environ. Sci.* **2008**, *1*, 134–138. [[CrossRef](#)]
9. Joó, F. Breakthroughs in hydrogen storage—formic acid as a sustainable storage material for hydrogen. *ChemSusChem* **2008**, *1*, 805–808. [[CrossRef](#)]
10. Sheet, S.D. Formic acid Formic acid. *ICIS Chem. Bus.* **2017**, *1*, 1–12.
11. Carra, S.; Santacesaria, E. Engineering Aspects of Gas-Liquid Catalytic Reactions. *Catal. Rev.* **1980**, *22*, 75–140. [[CrossRef](#)]
12. Stathi, P.; Solakidou, M.; Louloudi, M.; Deligiannakis, Y. From homogeneous to heterogenized molecular catalysts for H<sub>2</sub> production by formic acid dehydrogenation: Mechanistic aspects, role of additives, and co-catalysts. *Energies* **2020**, *13*, 733. [[CrossRef](#)]
13. Onishi, N.; Laurency, G.; Beller, M.; Himeda, Y. Recent progress for reversible homogeneous catalytic hydrogen storage in formic acid and in methanol. *Coord. Chem. Rev.* **2018**, *373*, 317–332. [[CrossRef](#)]
14. Coffey, R.S. The decomposition of formic acid catalysed by soluble metal complexes. *Chem. Commun.* **1967**, *18*, 923–924. [[CrossRef](#)]
15. Loges, B.; Boddien, A.; Junge, H.; Beller, M. Controlled generation of hydrogen from formic acid amine adducts at room temperature and application in H<sub>2</sub>/O<sub>2</sub> fuel cells. *Angew. Chemie Int. Ed.* **2008**, *47*, 3962–3965. [[CrossRef](#)] [[PubMed](#)]
16. Fellay, C.; Yan, N.; Dyson, P.J.; Laurency, G. Selective formic acid decomposition for high-pressure hydrogen generation: A mechanistic study. *Chem. A Eur. J.* **2009**, *15*, 3752–3760. [[CrossRef](#)] [[PubMed](#)]
17. Pan, Y.; Pan, C.L.; Zhang, Y.; Li, H.; Min, S.; Guo, X.; Zheng, B.; Chen, H.; Anders, A.; Lai, Z.; et al. Selective hydrogen generation from formic acid with well-defined complexes of ruthenium and phosphorus-nitrogen PN3-pincer ligand. *Chem. Asian J.* **2016**, *11*, 1357–1360. [[CrossRef](#)] [[PubMed](#)]
18. Boddien, A.; Mellmann, D.; Gärtner, F.; Jackstell, R.; Junge, H.; Dyson, P.J.; Laurency, G.; Ludwig, R.; Beller, M. Efficient dehydrogenation of formic acid using an iron catalyst. *Science* **2011**, *333*, 1733–1736. [[CrossRef](#)]
19. Stathi, P.; Deligiannakis, Y.; Louloudi, M. Co-catalytic enhancement of H<sub>2</sub> production by SiO<sub>2</sub> nanoparticles. *Catal. Today* **2015**, *242*, 146–152. [[CrossRef](#)]
20. Solakidou, M.; Deligiannakis, Y.; Louloudi, M. Heterogeneous amino-functionalized particles boost hydrogen production from Formic Acid by a ruthenium complex. *Int. J. Hydrogen Energy* **2018**, 21386–21397. [[CrossRef](#)]
21. Solakidou, M.; Theodorakopoulos, M.; Deligiannakis, Y.; Louloudi, M. Double-ligand Fe, Ru catalysts: A novel route for enhanced H<sub>2</sub> production from Formic Acid. *Int. J. Hydrogen Energy* **2020**, *45*, 17367–17377. [[CrossRef](#)]
22. Boddien, A.; Loges, B.; Junge, H.; Gärtner, F.; Noyes, J.R.; Beller, M. Continuous hydrogen generation from formic acid: Highly active and stable ruthenium catalysts. *Adv. Synth. Catal.* **2009**, *351*, 2517–2520. [[CrossRef](#)]
23. Mellone, I.; Gorgas, N.; Bertini, F.; Peruzzini, M.; Kirchner, K.; Gonsalvi, L. Selective Formic Acid Dehydrogenation Catalyzed by Fe-PNP Pincer Complexes Based on the 2,6-Diaminopyridine Scaffold. *Organometallics* **2016**, *35*, 3344–3349. [[CrossRef](#)]
24. Guan, C.; Zhang, D.D.; Pan, Y.; Iguchi, M.; Ajitha, M.J.; Hu, J.; Li, H.; Yao, C.; Huang, M.H.; Min, S.; et al. Dehydrogenation of Formic Acid Catalyzed by a Ruthenium Complex with an N,N'-Diimine Ligand. *Inorg. Chem.* **2017**, *56*, 438–445. [[CrossRef](#)] [[PubMed](#)]
25. Agapova, A.; Alberico, E.; Kammer, A.; Junge, H.; Beller, M. Catalytic Dehydrogenation of Formic Acid with Ruthenium-PNP-Pincer Complexes: Comparing N-Methylated and NH-Ligands. *ChemCatChem* **2019**, *11*, 1910–1914. [[CrossRef](#)]

26. Stathi, P.; Deligiannakis, Y.; Avgouropoulos, G.; Louloudi, M. Efficient H<sub>2</sub> production from formic acid by a supported iron catalyst on silica. *Appl. Catal. A Gen.* **2015**, *498*, 176–184. [[CrossRef](#)]
27. Mellmann, D.; Barsch, E.; Bauer, M.; Grabow, K.; Boddien, A.; Kammer, A.; Sponholz, P.; Bentrup, U.; Jackstell, R.; Junge, H.; et al. Base-free non-noble-metal-catalyzed hydrogen generation from formic acid: Scope and mechanistic insights. *Chem. A Eur. J.* **2014**, *20*, 13589–13602. [[CrossRef](#)]
28. Boddien, A.; Loges, B.; Gärtner, F.; Torborg, C.; Fumino, K.; Junge, H.; Ludwig, R.; Beller, M. Iron-catalyzed hydrogen production from formic acid. *J. Am. Chem. Soc.* **2010**, *132*, 8924–8934. [[CrossRef](#)]
29. Sánchez-De-Armas, R.; Xue, L.; Ahlquist, M.S.G. One site is enough: A theoretical investigation of iron-catalyzed dehydrogenation of formic acid. *Chem. A Eur. J.* **2013**, *19*, 11869–11873. [[CrossRef](#)]
30. Yang, X. Mechanistic insights into iron catalyzed dehydrogenation of formic acid:  $\beta$ -hydride elimination vs. direct hydride transfer. *Dalt. Trans.* **2013**, *42*, 11987–11991. [[CrossRef](#)]
31. Léval, A.; Agapova, A.; Steinlechner, C.; Alberico, E.; Junge, H.; Beller, M. Hydrogen production from formic acid catalyzed by a phosphine free manganese complex: Investigation and mechanistic insights. *Green Chem.* **2020**, *22*, 913–920. [[CrossRef](#)]
32. Mellone, I.; Bertini, F.; Peruzzini, M.; Gonsalvi, L. An active, stable and recyclable Ru(II) tetraphosphine-based catalytic system for hydrogen production by selective formic acid dehydrogenation. *Catal. Sci. Technol.* **2016**, *6*, 6504–6512. [[CrossRef](#)]